COMPUTATION OF WINDING FAULT IN DISC-TYPE TRANSFORMER WINDING

Usha KrishnaKumar, Jyotirmayee Dash, and Usa Savadamuthu
Division of High Voltage Engineering
Department of Electrical and Electronics Engineering, Anna University, Chennai, India
ushaeee@yahoo.co.in

Abstract**:** *In this paper, an attempt has been made to analyse the frequency response of transformer winding under healthy and faulty conditions (inter-disc short) when very fast transient overvoltages(VFTOs) invades the transformer winding. An algorithm using hybrid model has been developed to incorporate inter–disc faults at different locations of the winding in the transmission line model with frequency dependent loss factor. The resonant frequencies under healthy and faulty conditions are measured using Sweep Frequency Response Analyser. Simulation and measurements are performed on a 22kV prototype continuous disc winding and efficacy of the model is verified by the application of Pearson's Correlation Coefficient in frequency domain. Interturn voltages are computed using hybrid model under healthy and faulty conditions.*

Key words: *GIS, Interdisc Faults, MTL, Transformer Insulation and VFTO.*

1. Introduction

Gas insulated substation (GIS) has gained a wide range of acceptance in power system for its compactness and high reliability. Switching operations of disconnector switch and circuit breaker within GIS generates very fast transient over voltages (VFTOs), which are characterized by a very short rise-time of less than 0.1 μs and amplitude of 2.5 p.u. and an oscillatory component of several MHz lasting for tens of micro seconds [1-4]. VFTO could cause oscillations in the voltage inside the transformer connected directly to GIS, since high frequency surges travel more easily along the coaxial gas insulated bus. Resonance may occur in transformer winding when the frequency of incoming VFTO matches some of the resonant frequencies of the transformer [2]. Due to very short rise time, it can cause an unbalance in voltage distribution in transformer windings. Under these circumstances, the turn-to-turn voltage can rise close to the transformer basic insulation level. The VFTOs produced by switching in GIS depends not only on the connection between the GIS and transformer, but also on the transformer parameters and type of the winding [5]. To predict the transient behaviour of the transformer under different types of overvoltages, several models have been reported in the literature. The various techniques of lumped parameter models are presented in [6-9]. As the efficacy of the model depends on the range of the frequency, it has been reported that the RLC ladder network model can be used for the transients in the frequency range of 10kHz - 1MHz and Transmission Line Model for 1MHz - 5MHz [10].Detailed survey of transformer failure report shows that more than fifty percent of the failures in power transformers are due to the insulation failures in windings [11].

Most of the insulation failures are due to overvoltages of different waveshapes ranging from lightning impulse to VFTO. Computation of interturn voltages in transformers is of great importance for the design of transformer insulation. VFTO can result in higher interturn voltages than the overvoltages produced by lightning impulse waves defined by the standards [12]. As the effect of VFTO on transformer winding under healthy and faulty conditions is more severe when compared to lightning impulses, it becomes necessary to use an appropriate model which can simulate winding faults under VFTO. Inter–disc faults at different locations of the winding is analysed in the transmission line model with frequency dependent loss factor. Frequency Response Analyzer(FRA) results are sensitive to a variety of winding faults and are presumed to be less dependent on previous reference measurements[13]. By using Sweep frequency response analyser (FRAX 101, Megger), measurement of the resonant frequencies under healthy and faulty conditions are performed on the 22kV prototype continuous disc winding and the interturn voltages are computed.

2. Transmission - Line Models

2.1 Single transmission-line model

In this model, each coil is considered as a transmission line. Fig. 1 shows STLM for one-coil system [1]. A sinusoidal voltage of amplitude E_o and angular frequency ω is applied to the transformer consisting of a single N-turn coil. The average length of each turn in the coil is taken as 'a' and the line length is l=a*N. The distributed constants C_0 and

C_1 represent the capacitance between the static plates.

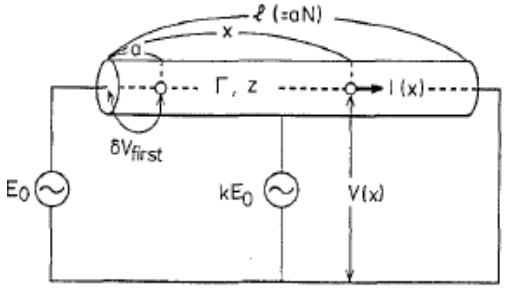

Fig. 1. Single transmission-line model for one-coil system

The following circuit equation is obtained from Fig. 1.

$$\frac{d(V(x))}{dx} = -j\omega[L](I(x)) \tag{1}$$

$$\frac{d(I(x))}{dx} = -j\omega[C](V(x)) + j\omega(C_o)E_o \tag{2}$$

where vectors (V(x)) and I(x)) respectively, denote the voltage and current of the coil, and the inductance and capacitance matrices [L] and [C] respectively are of distributed constants.

The capacitance matrix C is formed as follows:

Ci,i - capacitance of turn 'i' to ground and sum of all other capacitances connected to turn 'i';

Ci,j - capacitance between turns 'i' and 'j' taken with the negative sign.

The inductance matrix L is calculated through the capacitance matrix C.

$$[L][C] = \frac{1}{v_s^2} \tag{3}$$

where, vs is the velocity of wave propagation. From the electromagnetic point of view travelling wave propagates through the inter-turn space.

Hence v_s is calculated as

$$v_s = \frac{C}{\sqrt{\varepsilon_r}} \tag{4}$$

where, C is the speed of light and €r is the dielectric constant of the transformer insulation. It is pointed out that the matrix in (3) takes into account the mutual inductances within a specific coil.

Substituting equation (3) in equation (1) yields

$$\frac{d^2(V(x))}{dx^2} = \Gamma^2\{(V(x)) - kE_O\} \tag{5}$$

Here, $k = \frac{C_o}{C_o + C_1}$ indicates the electrostatically induced voltage ratio, G is the propagation constant in the wave equation (5).The pure imaginary G corresponds to loss free propagation. The solution for eqn. (5) is given by

$$V(x) = k_i E_0 + A_i e^{-\Gamma x} + B_i e^{\Gamma x} \tag{6}$$

$$I(x) = 1/Z\left(Ae^{-\Gamma x} - Be^{\Gamma x}\right) \tag{7}$$

The first term in equation (6) represents the electro statically induced voltage. In equation (7), Z is the characteristic impedance of a turn in a coil defined by

$$Z_i \cong \frac{1}{\upsilon_s\left(C_o + C_1 + K\left(1 - \cos\left(\frac{\omega a}{\upsilon_s}\right)\right)\right)} \tag{8}$$

In equation (8), K is the inter-turn capacitance of the coil, ω is the angular frequency of the sinusoidal voltage applied to the transformer coil and a represents the length of a single turn in the coil. Utilizing the complex dielectric constant and the complex distance reflecting the proximity effect, the following form of Γ is derived:

$$\Gamma = \frac{1}{Vs * d}\sqrt{\frac{w}{2\sigma\mu}} + w\frac{\tan\delta}{2Vs} + \frac{jw}{Vs} \tag{9}$$

where σ is the conductivity of the conductor, μ is the magnetic permeability and d is the distance between the conductors.

The values of A and B in eqns. (6) and (7) are determined from the boundary condition V(0) =E0 ; V(l) = 0; Using these values, equations (6) and (7) give the voltage and current distribution in the coil.

The advantage of STLM is that the whole length of the coil is considered as one line and the voltages and currents in the coil are computed by solving a minimal number of equations.

2.2 Multi-conductor transmission- line model

MTLM uses the determined voltages in frequency domain from the STLM. Neglecting the magnetic flux in the core, the multi-conductor system without a core is shown in Fig. 2 employed as in [1].

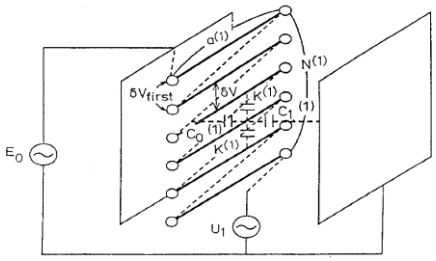

Fig.2. Multi-conductor transmission line model for one coil system.

The solution of the multi-conductor transmission-line model is similar to that for a single transmission line model given by eqns. (6) and (7).

$$V_i(x) = kE_0 + A_i e^{-\Gamma x} + B_i \tag{10}$$

$$I_i(x) = 1/Z_i\left(Ae^{-\Gamma x} - Be^{\Gamma x}\right) \tag{11}$$

The system of equations (10) and (11) is used to compute the voltages and currents in the turns of a particular coil. The values of A_i and B_i are determined by the boundary conditions:

$$\mathbf{V_1(0) = E_o;} \qquad \mathbf{V_N(a) = 0;}$$

$$\mathbf{V_i(0) = V_{i-1}\,(a);} \qquad \mathbf{I_i(0) = I_{i-1}(a);}$$

This is a set of 2N equations for the same number of unknowns Ai and Bi. The matrix equation from which the vectors Ai and Bi can be determined is

$$\begin{bmatrix} MA & MB \\ MC & MD \end{bmatrix} \begin{bmatrix} A \\ B \end{bmatrix} = \begin{bmatrix} (E)_{N+1} \\ (0)_{N-1} \end{bmatrix} \tag{12}$$

In eqn. (12), (E) represents the excitation vector.

The description of the matrix elements is given in [2]. The matrix must be solved for each step frequency by providing the voltages at the beginning of the each coil which were previously determined by the STLM. The interturn voltage is defined as the difference between the voltages of two adjacent turns in a coil. The interturn voltage is obtained by dV = Vi(x) – Vi+1(x), where Vi is the voltage in the ith turn of the studied coil.

The matrices MC, MD in equation (12) can be determined if [C] matrix is known. [C] Matrix can be computed using the following simple form. The values of Γ and z_i can be evaluated from K, C_0, C_1 using equations (8) and (9). K can be easily obtained from the insulation dimension and the rest can be determined from the coil capacitances C_m and C_g as shown in Fig. 3 in the following way.

$$[C] = \begin{bmatrix} (C_0+C_1+K) & -K & 0 & \dots & 0 \\ -K & (C_0+C_1+2K) & -K & \dots & \dots \\ 0 & -K & \dots. & \dots & 0 \\ . & & & & \\ . & \dots. & \dots. & \dots. & 0 \\ . & & \dots. & (C_0+C_1+2K) & -K \\ 0 & . \ . \ . & & -K & (C_0+C_1+K) \end{bmatrix} \tag{13}$$

ki indicates the capacitively distributed voltages among the coils, expressed as,

$$K_i = \Pi_{j=1}^{i} \frac{C_L^{(j-1)}}{C_L^{(j)} + C_g^{(j)}} \tag{14}$$

$C_L^{(i)}$ and $C_H^{(i)}$ have been shown in Fig. 3. The total capacitance of coil i is given by $C_H^{(i)} + C_L^{(i)} + C_g^{(i)}$ The equivalent capacitance along the length of the disc l_i should be divided by the ratio k_i:(1-k_i) to determine C_o(i) and C_1(i)

$$C_0^{(i)} = k_i * \left(C_H^{(i)} + C_L^{(i)} + C_g^{(i)}\right)/l_i \tag{15 a}$$

$$C_1^{(i)} = (1-k_i) * \left(C_H^{(i)} + C_L^{(i)} + C_g^{(i)}\right)/l_i \tag{15 b}$$

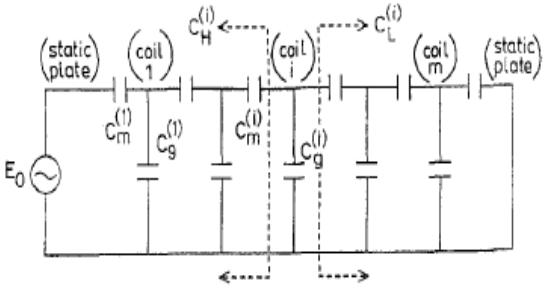

Fig. 3. Equivalent capacitive network of a winding.

3. MTL Model of 22kV Prototype Disc Winding

A small change in the parameters can cause significant difference in the results while studying the transient behaviour of the transformer winding under VFTOs. The algorithm of the transmission line model is modified without static plates and a 22kV disc winding is analyzed by using modified algorithm. The physical dimensions and dissipation related constants of the coil are given in Table 1. Fig. 4 shows the capacitive voltage distribution among the coils of disc winding. Dielectric loss factor in unimpregnated kraft paper is affected by the change of the test frequency.

Table 1
Constants of 22 kV disc winding

Turn Length (a)	1m
Number of turns (N)	12
Number of discs (Nc)	40
Dielectric constant of insulation (εr)	2.08
Distance between the conductor (d)	0.3125mm
Conductor conductivity (σ)	5 x 10^{7} S/m
Permeability (μ=μo)	4πx10^{-7} H/m
Surge velocity (υs)	208 m /μs
Dielectric loss factor (tan δ)	0.02
Coil capacitance (Cm)	2.23pF
Ground Capacitance (Cg)	11.65pF
Interturn Capacitance (K)	147.8pF

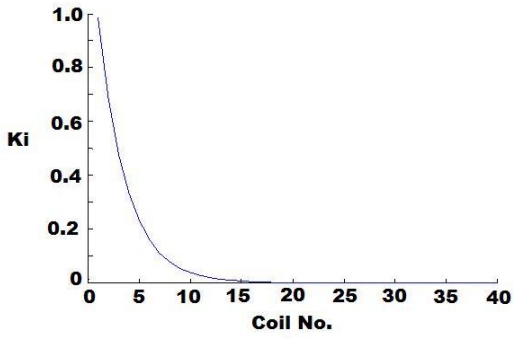

Fig. 4. Capacitive voltage distribution

The dielectric constant when measured at lower permissible test temperature, demonstrates its highest variation as the test frequency is increased. At 25^{0}C, the loss factor can be estimated as 0.005 in the frequency band of 0–10 kHz and then it increases with frequency and at 1 MHz it is equal to 0.056[14]. Assuming a drooping variation of transformer insulation loss factor with frequency in the frequency band of 1Mhz - 25Mhz, a special type of variation, is employed. These variations can introduce a significant change, especially on the response of the model

4. Analysis of Healthy Winding

4.1 Frequency Domain Analysis

The voltage distribution of 22 kV disc winding is computed by MTL model. Continuous disc winding has 40 discs and each disc has 12 turns in it. The schematic diagram of the disc winding is shown in the Fig. 5. Tappings were brought out at every 4 disc (4 disc is 10% of the winding) and 2 disc (2.5% of the winding) in order to create inter disc short fault.

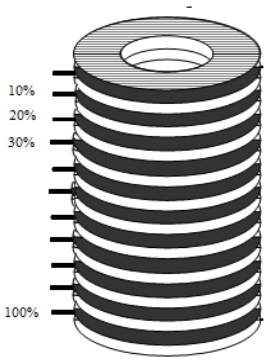

Fig. 5. Schematic diagram of the disc winding

Frequency characteristic of voltage across coil 5 and coil 9 are shown in Fig. 6 and Fig. 7 respectively. In the figure, (a) and (b) represents the measured value and the simulated value respectively. Fig. 8 shows the frequency characteristics of dV12 of the first coil.

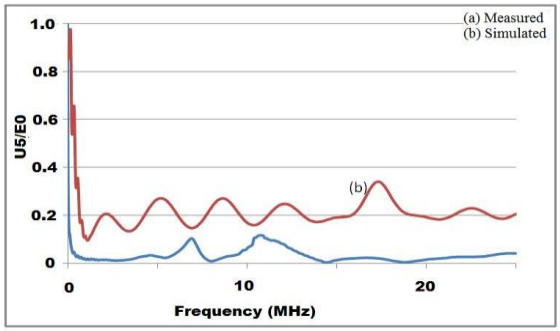

Fig. 6. Frequency characteristic of voltage across coil 5

The resonant frequencies are 1.4, 8.45, 9.4 and 18.88 MHz. Thus the first coil is analyzed in time domain to determine the inter-turn voltage distribution at its resonant frequency (1.4MHz).

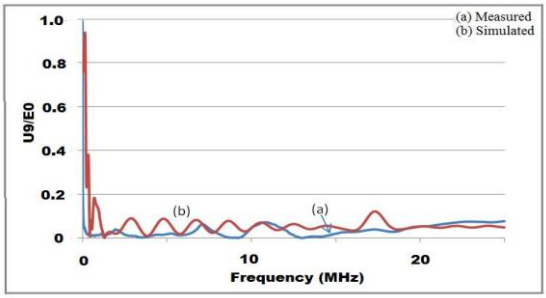

Fig. 7. Frequency characteristic of voltage across coil 9

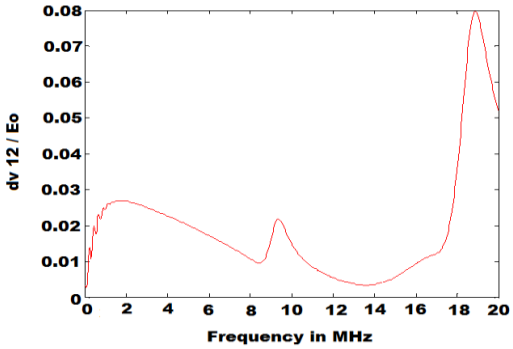

Fig. 8. Frequency characteristics of interturn voltage of coil 1

4.2 Verification Using Pearson's Correlation Coefficient

Correlation is a useful technique to investigate the relationship between two quantitative, continuous variables. It measures the strength and direction of a linear relationship between two variables. This correlation coefficient is presented by the following equation:

$$r = \frac{\Sigma_{i=1}^{n}\left(U_{mi} - \bar{U_m}\right)\left(U_{si} - \bar{U_s}\right)}{\sqrt{\Sigma_{i=1}^{n}\left(U_{mi} - \bar{U_m}\right)^2\left(U_{si} - \bar{U_s}\right)^2}} \quad (16)$$

where Um is the measured value of variable and Us is its simulated value. r could be a number between -1 and 1.A positive value of r means a positive linear relationship; a negative value of r means a negative linear relationship. The correlation is ideal as r approaches 1 and it is not desirable to approach -1 [7]. Considering the results shown in Table 2 the accuracy of the MTL model can be studied.

Table 2
Pearson's correlation coefficient for MTL model for healthy winding

Disc No.	tanδ const (0.02)	tanδ varying
1	0.254	0.254
2	0.761	0.764
5	0.622	0.625
9	0.489	0.494
13	0.393	0.4
17	0.311	0.32
21	0.23	0.24
25	0.156	0.168
29	0.07	0.084
Average	0.365	0.372

Due to the nonlinearity in voltage distribution as shown in Fig. 3 the coefficient has been shown upto only 70% of the winding. A relatively good correlation observed between the computed and measured voltages with frequency-dependent loss factor.

4.3 Time Domain Analysis

Utilizing the results of the frequency domain analysis, the transients initiated by a VFTO pulse of any waveform can be calculated using Inverse Fast Fourier Transform. The inter-turn voltages in frequency domain are calculated by multiplying the transfer function with the source function.

$$dV(j\omega) = H(j\omega)\, E_o(j\omega) \quad (17)$$

It is shown in [15] that the transfer function of a transformer may be regarded as a 'signature" of the transformer and is independent of the waveform applied. From equation (17), it can be seen that the transfer function H(jώ) is equal to the inter-turn voltage when the input is unity. This approach is used to calculate transfer function.

If the transformer is subjected to the following oscillating pulse representing an oscillatory VFTO pulse e(t) = sin ώpt ,then the frequency of the defined pulse is equal to the resonant frequency of a specific coil. (ώp = $2pf_o$, where f_o is the resonant frequency of the studied coil). The computed interturn voltage distribution in turns 1-2 of the first coil is shown in Fig. 9.

Reference [2] shows that the maximum interturn withstand voltage level is 1.5% of the source voltage.It is observed that the maximum amplitude of the computed interturn overvoltages at the resonant frequency is approximately 4.25% of the source voltage.

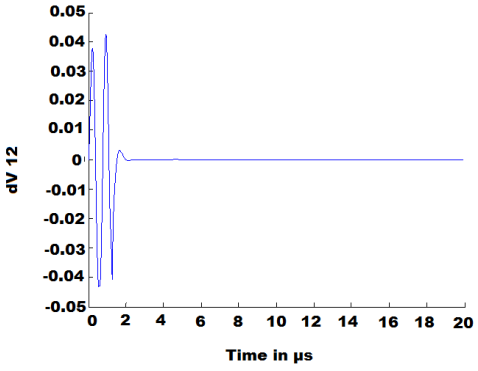

Fig. 9. Interturn voltage between turns 1&2 of coil 1

5. Analysis of Interdisc Fault Winding

5.1 Frequency Domain Analysis

Interdisc shorts are created at different positions of the disc winding. The voltage distribution of 22kV disc winding with fault is computed by MTL model.

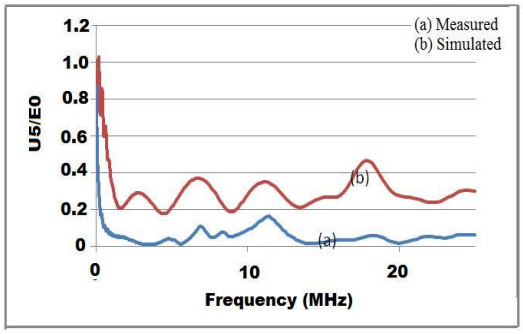

Fig. 10. Frequency characteristics of coil 5 with 2.5% fault

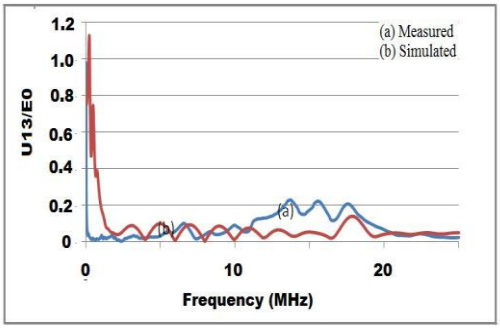

Fig. 11. Frequency characteristics of coil 13 with 10% fault

Voltages at different disc terminals are simulated and measured by means of Sweep frequency response analyser (FRAX 101, Megger). Fault of 2.5% of the winding is done by shorting the first and second disc. Fault of 10% and 20% of the winding are done by shorting first to fifth disc and first to ninth respectively.

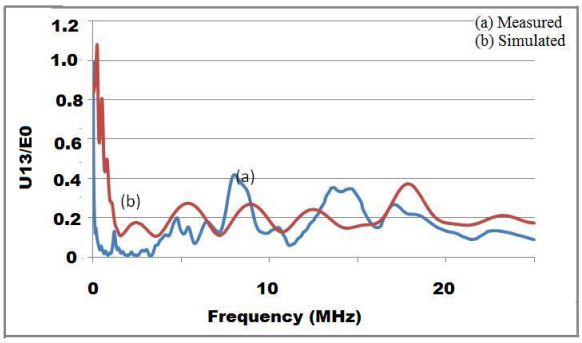

Fig. 12. Frequency characteristics of coil 13 with 20% fault

The voltage distribution in coil 5 with 2.5% of winding shorts is shown Fig. 10.The voltage distributions in coil 13 with 10% and 20% of winding shorts are shown in Fig. 11 and Fig. 12 respectively.

Table 3
Pearson's correlation coefficient for MTL model for inter disc fault winding

Fault / Disc	2.5%	10%	20%	30%
5	0.792	-	-	-
9	0.522	0.592	-	-
13	0.394	0.427	0.552	-
17	0.299	0.315	0.382	0.517
21	0.202	0.211	0.251	0.328
25	0.123	0.125	0.152	0.197
29	0.031	0.028	0.043	0.076
Average	0.338	0.283	0.276	0.28

There is good agreement between measured and simulated value. Table 3 shows Pearson's correlation coefficients for different percentage of faults in which the coefficients are taken between the measured and simulated value at different discs.

Table 4
Shift in resonant frequencies of coil 13 with 2.5% fault

Measured resonant frequency using SFRA (MHz)			Simulated resonant frequency using MATLAB (MHz)		
Healthy	2.5% Fault	% Shift	Healthy	2.5% Fault	% Shift
0.347	0.359	3.34	0.376	0.381	1.33
1.67	1.93	13.47	1.74	2	13
2.67	3.06	12.74	2.64	2.92	9.6
3.94	4.03	2.2	3.44	3.77	8.75
4.53	4.63	2.1	4.13	4.48	7.8
5.5	5.57	1.25	5.51	5.97	7.7
6.69	6.77	1.18	6.8	7.1	4.22
8.05	8.53	5.6	8.24	8.93	7.7
9.68	9.79	1.12	9.68	10.4	6.9

With fault, resonant frequencies of the transformer are getting shifted. Table 4 and 5 shows the shift in resonant frequencies of coil 13 with 2.5% and 10% of fault respectively.

Table 5
Shift in resonant frequencies of coil 13 with 10% fault

Measured resonant frequency using SFRA (MHz)			Simulated resonant frequency using MATLAB (MHz)		
Healthy	10% Fault	% Shift	Healthy	10% Fault	% Shift
0.184	0.19	3.16	0.193	0.21	9.81
0.347	0.364	4.67	0.32	0.33	4.76
0.417	0.437	4.58	0.427	0.46	7.78
1.68	2.46	18.45	1.7	2.07	17.9
2.66	2.9	8.28	2.8	3.15	11.1
4.63	5.02	7.77	4.8	5.02	4.38
7.6	7.9	3.80	7.6	7.96	4.52
10.9	11.2	2.68	10.3	11	6.36

5.2 Time Domain analysis

Fig. 13 shows the simulated inter-turn voltages in turn 1-2 in coil 6 under healthy and faulty condition of 10%winding short fault. It is observed that the inter-turn voltage rises to 3.386% of input voltage with 10% of winding being shorted instead of 1.38% in healthy condition. Fig. 14 shows simulated dV12 in coil 10 under healthy as well as faulty condition with disc 1-5 and 5-9 faults. It has been shown that inter-turn voltage is 0.58% under healthy condition where as it rises to 1.17% with disc 5-9 short and to 1.57% with 1-5 short.

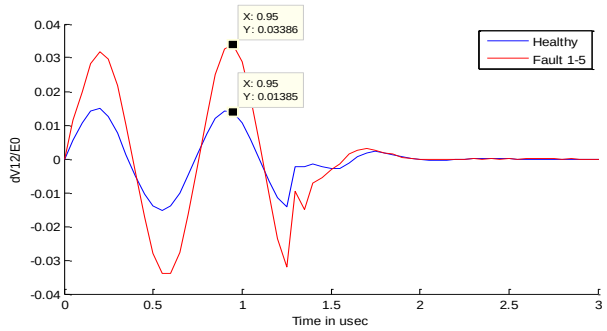

Fig.13. Interturn voltage in turn 1-2 for coil 6

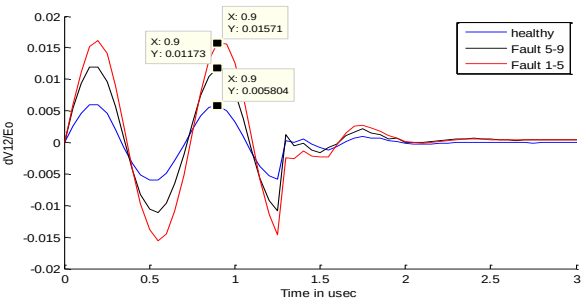

Fig.14. Interturn voltage in turn 1-2 for coil 10

6. Conclusion

This paper presents the interdisc fault analysis of a 22kV prototype continuous disc winding using MTL model for very fast transient studies and the simulation results have been compared with the measurement results. The efficacy of the model is verified by the application of Pearson's Correlation Coefficient in frequency domain. A relatively good correlation observed between measurement and MTL model with a frequency-dependent loss factor variation, provides a better agreement between the computed and the measured voltages. It has been shown that there will be minimum shift of 1.2% in resonant frequencies with 2.5% fault and 2.68% with 10% fault compared to healthy condition. By computation, it has been observed that the interturn voltage is higher with inter-disc fault at initial position of the winding when compared to the fault at other locations of the winding.

Reference

[1] Shibuya Y, Fujita S and Hosokawa N.: *Analysis of very fast transient over voltage in transformer winding*. In: IEEE Proce.-Gener, Transm. Distrib, Vol.144, No.5, September 1997.

[2] Marjan Popov, Lou van der sluis,Gerardus S.Paap and Hans De Herdt.: *Computation of Very Fast Transient Over voltages in Transformer Windings*. In: IEEE transactions on power delivery vol.18,No.4.October 2003

[3] Shibuya Y, Fujita S and Tamaki E.: *Analysis of very fast transients in transformers*. In: IEE Proc. - Gener. Transm. Distrib., Vol.148,No.5, September 2001.

[4] Shibuya Y, Fujita S and Hosokawa N.: *Experimental Investigation of High Frequency Voltage Oscillation in Transformer windings*. In: IEEE Transactions on Power Delivery, Vol.13,No.4,October 1998

[5] Guishu Liang, Haifeng Sun, Xile Zhang and Xiang Cui.: *Modeling of Transformer Windings Under Very Fast Transient Over voltages*. In: IEEE Transactions on Electromagnetic Compatibility, Vol.48,No.4, November 2006.

[6] R. C. Degeneff, W. J. McNutt, W. Neugebauer, J. Panek, M. E. Mc-Callum, and C. C. Honey.: *Transformer response to system switching voltage*. In: IEEE Trans. Power App. Syst., vol. PAS-101, no. 6, pp.1457–1470, Jun. 1982.

[7] M. Gutierrez, R. C. Degeneff, P. J. McKenny, and J. M. Schneider.: *Linear lumped parameter transformer model reduction technique*. In: IEEE Trans. Power Del., vol. 10, no. 2, pp. 853–861, Apr. 1995.

[8] M. Gutierrez, R. C. Degeneff, and P. J. McKenny.: *A method for constructing reduced order models for system studies from detailed lumped parameter models.* In: IEEE Trans. Power Del., vol. 7, no. 2, pp. 649–655,Apr. 1992.

[9] R. C. Dugan, R. Gabrick, J. C. Wright, and K. V. Pattern.: *Validated techniques for modeling shell-form EHV transformers*. In: IEEE Trans.Power Del., vol. 4, no. 2, pp. 1070–1078, Apr. 1989.

[10] Hassan Hosseini, Mehdi Vakilian, and Gevork B. Gharehpetian.: *Comparison of Transformer Detailed Models For Fast and Very Fast Transient Studies*. In: IEEE Trans. Power Deliv., 2008, 23, (2), pp. 733–741 2008.

[11] CIGRE JWG 12/13/23.21 (2002).: *Electrical Environment of Transformers*. In: Paris.

[12] Gerben Hoogendorp , Marjan Popov and Lou van der Sluis.: *Application of Hybrid Modeling for Calculating Interturn Voltages in Transformer Windings*. In: IEEE transactions on power delivery, vol. 24, no. 3, july 2009.

[13] Prameela M. G. Radhakrishna Murthy Pradeep Nirgude B. Gunasekara.: *Experimental Investigations to Identify SFRA Measurement Sensitivity for Detecting Faults in Transformers*. In: 16th National power systems conference, 15th-17th December, 2010.

[14] F.M. Clark.: *Insulating Materials for design and Engineering Practice*. In: New York: Wiley, 1962, vol.1,pp 275.

[15] Syed M. Islam & Gerard Ledwich.: *Locating Transformer Faults Through Sensitivity Analysis of High Frequency Modeling Using Transfer Function Approach*. In: Conference Record of the 1996 IEEE International Symposium on Electrical Insulation, Montreal, Quebec, Canada, June 16-19,1996.